

We are IntechOpen, the world's leading publisher of Open Access books Built by scientists, for scientists

6,900

Open access books available

186,000

International authors and editors

200M

Downloads

Our authors are among the

154

Countries delivered to

TOP 1%

most cited scientists

12.2%

Contributors from top 500 universities



WEB OF SCIENCE™

Selection of our books indexed in the Book Citation Index
in Web of Science™ Core Collection (BKCI)

Interested in publishing with us?
Contact book.department@intechopen.com

Numbers displayed above are based on latest data collected.
For more information visit www.intechopen.com



Multiple Person Localization Based on their Vital Sign Detection Using UWB Sensor

Dušan Kocur, Daniel Novák and Mária Švecová

Additional information is available at the end of the chapter

<http://dx.doi.org/10.5772/66361>

Abstract

In the past period, great efforts have been made to develop methods for through an obstacle detection of human vital signs such as breathing or heart beating. For that purpose, ultra-wideband (UWB) radars operating in the frequency band DC-5 GHz can be used as a proper tool. The basic principle of respiratory motion detection consists in the identification of radar signal components possessing a significant power in the frequency band 0.2–0.7 Hz (frequency band of human respiratory rate) corresponding to a constant bistatic range between the target and radar. To tackle the task of detecting respiratory motion, a variety of methods have been developed. However, the problem of person localization based on his or her respiratory motion detection has not been studied deeply. In order to fill this gap, an approach for multiple person localization based on the detection of their respiratory motion will be introduced in this chapter.

Keywords: emergency events, person localization, respiratory motion, signal processing, ultra-wideband (UWB) sensor/radar, vital signs detection of persons

1. Introduction

At the beginning of the twenty-first century, the human society faced quite a number of specific social trends. The increasing density of population of towns and town agglomerations, criminality growing and political tensions producing terrorism, and growth of the percentage of elder people can be ranked among them.

A high density of the population at emergency events such as earthquakes or building collapses results in a high number of injured and trapped persons. At these disasters, many persons can survive the most critical moments. However, they have often limited capability of the motion or they are unconscious, what makes more difficult to save them. There is,

however, necessary to emphasize that the capability and rapidity of the victim localization is the most critical for their lifesaving.

People localization is very important not only for post-disaster rescue but also for military and security operations [1]. Here, reservoirs, power plants, and other critical infrastructures are extremely vulnerable to terrorist attack. Therefore, the request for monitoring of the mentioned critical areas and for the detection of unauthorized intrusion is still needed. The information about the number of persons and their positions can be very useful for security troops to take the right decisions. In the case of the mentioned disasters and law enforcement operations, people to be detected and localized are often situated behind nonmetallic obstacles (e.g. walls). That is the reason why conventional sensors (e.g. cameras) cannot be applied for person monitoring for such scenarios.

It is expected that the number of seniors will increase in the future. It will result in dramatic challenges to the society since elder people need additional care and assistance. It is well known that many people aged above 65 years fall down in their dwelling every year and above 3% of them are not able to rise again without external help. They have to stay in their uncomfortable situation over hours or even days before they get help. As a result, a number of people are dying in consequence of such accidents [2]. In order to save life of the seniors, they can be monitored, for example, by conventional cameras. However, this simple solution represents a serious invasion to their private life, and hence it is not well accepted. On the other hand, a solution enabling to localize seniors at their home taking into account their privacy and at the same time detection of emergency events is really very needful. It has been shown in Ref. [2] that ultra-wide frequency band radars (UWB sensors) can provide solutions of the outlined problem.

The analyses of the requirements for person localization according to above outlined scenarios have shown that short-range high-resolution radars emitting electromagnetic waves with ultra-wide frequency band (UWB radars) using relatively low frequencies can be used with advantage for such applications. The exploitation of the ultra-wide frequency band provides the high resolution of the radar. On the other hand, the electromagnetic waves emitted in the frequency band DC-5GHz can penetrate through standard building materials (e.g. wood, concrete, bricks, etc.) with acceptable attenuation. Therefore, UWB sensors employing this frequency band are capable to detect a target situated not only for line-of-sight but also for a target located behind a nonmetallic obstacle. Moreover, UWB radar systems can be constructed to be lightweight and small.

UWB radars could be available as handheld sensor systems consisting of antenna system, radio frequency (RF) block, analog-to-digital (AD) convertors, and digital circuitry including a computer and software. On the other hand, UWB sensors provide also privacy requested at people monitoring at their home, and hence they can be implemented as a part of complex sensor networks applied for senior monitoring in ambient-assisted living (AAL) programs as well.

The key part of the UWB sensor system software consists in the implementation of UWB radar signal processing procedure intent on human being detection, localization, and tracking. The

deeper analyses of person detection using UWB sensors have shown that it is necessary to distinguish between the detection of moving and static persons. In this context, a person moving within the monitored area in such a way that their coordinates are changing is referred to as a moving person. On the other hand, a living person is considered as static person, if he or she is situated but not moving within the monitored area in such a way that their coordinates are changing. Then, while a typical form of moving person movement is, for example, his or her walking or running, typical forms of static person movement are his or her respiration motions or heart beating, which is commonly referred to as person's vital signs. As examples of static persons, unconscious person located beneath the rubble of the building or avalanche, bound people (prisoners of terrorists) and sleeping persons, and so on can be given.

In this chapter, we focus on UWB radar signal processing procedure for localization of static persons situated behind a nonmetallic obstacle. First, we state the basic principle of the static person detection based on the detection of his or her respiratory motions. Then, the state-of-the-art of UWB radar signal processing concerning static person detection and localization will be presented in Section 3. The core of the chapter will be presented in Section 4. Here, a Welch periodogram method for multiple static person localization based on their vital sign detection will be given. As the vital signs, person respiratory motions (breathing) will be considered. The particular phases of this method will be illustrated by corresponding experimental results. Finally, some conclusions will be summarized in Section 5.

2. Respiratory motion detection: problem statement and its fundamental solution

Figure 1 symbolizes the generic measurement arrangement illustrating the basic principle of respiratory motion detection [2]. A transmitting antenna T_x converts the signal $p(t, \tau)$ into an electromagnetic wave, which propagates toward the body of the person. There, it will be partially reflected and travels back to the receiving antenna R_x , which converts the wave back into signal $r(t, \tau)$ that has to be captured by appropriate radar electronics. Then, the radar device converts the received signals by a proper pulse compression method into impulse responses $h(t, \tau)$ of the environment through which the signal emitted by the radar is

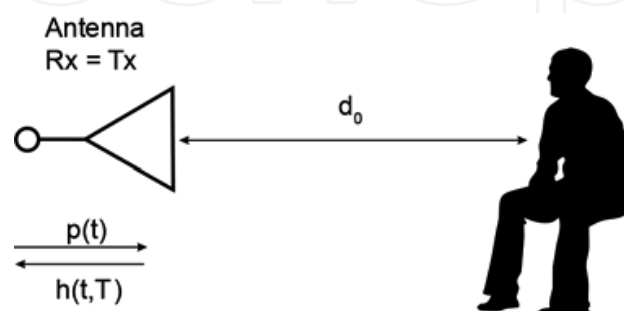


Figure 1. Basic measurement arrangement.

propagated. The variables t and τ , and the set of $h(t, \tau)$ represent fast-time (propagation time), slow-time (observation time), and raw radar data usually referred to as radargram, respectively.

Let us assume for this moment that the same antenna is used for the signal transmission and reception, and a static person is located in front of this antenna in the distance d_0 . Under such conditions, signal $h(t, \tau)$ can be expressed as follows [2, 3]:

$$h(t, \tau) = \sum_{i=1}^N A_i p(t-t_i) + A_0 p(t-t_d(\tau)) = h_b(t, \tau) + h_0(t, \tau). \quad (1)$$

In this expression, the constant term A_i stands for the path gain (or loss) of the i th signal path. The signal components $A_i p(t-t_i)$ for $i \neq 0$ represent the reflections of the transmitted signal from static objects (i.e. not reflections due to static person). Then,

$$h_b(t, \tau) = \sum_{i=1}^N A_i p(t-t_i) \quad (2)$$

is the component of $h(t, \tau)$ representing static clutter and noise (e.g. noise due to antenna and other electronic components of radar device, etc.). On the other hand, signal

$$h_0(t, \tau) = A_0 p(t-t_d(\tau)) \quad (3)$$

expresses the component of $h(t, \tau)$ due to static persons. The time delay $t_d(\tau)$ (associated with vital signs) represents the time of arrival (TOA) of the static person. It covers the time signal required to travel across *Tx-target-Rx* trajectory. The time delay $t_d(\tau)$ varies depending on the distance of the target from the antenna system. Slight but periodic changes of TOA are caused by a movement of the target chest due to periodical chest movement caused by breathing process (with a frequency f_b) and heartbeats (with frequency f_h) [2, 3]. Then, $t_d(\tau)$ can be approximately expressed as

$$t_d(\tau) = 2d(t_0, \tau)/c \quad (4)$$

where $c = 3 \times 10^8 \text{ ms}^{-1}$ is the speed of light and

$$d(t_0, \tau) = d_0 + m_b(\tau) + m_h(\tau) = d_0 + m_b \sin(2\pi f_b \tau) + m_h \sin(2\pi f_h \tau) \quad (5)$$

$$m_b(\tau) = m_b \sin(2\pi f_b \tau) \quad (6)$$

$$m_h(\tau) = m_h \sin(2\pi f_h \tau) \quad (7)$$

The term $d_0(t_0, \tau)$ is a component expressing the reflection from static object situated in distance d_0 from the radar antenna, and m_b and m_h are the breathing and heart amplitude, respectively. The peak-to-peak thorax motion due to breathing of an adult person ranges from 4 to 12 mm, while the peak-to-peak motion due to the heartbeat is about 0.5 mm. Then, $m_b \gg m_h$ and the signals $d(t_0, \tau)$ and $t_d(\tau)$ can be expressed as

$$d(t_0, \tau) \approx d_0 + m_b \sin(2\pi f_b \tau) \quad (8)$$

$$t_d(\tau) = 2d(t_0)/c + (2m_b/c) \cdot \sin(2\pi f_b \tau). \quad (9)$$

Within a long-term observation, breathing can be qualified as a periodic process with its own frequency f_b . According to [4], this frequency can take values from 0.2 Hz caused by slow, calm breathing up to 0.7 Hz caused by fast, stressful breathing. Then, taking this knowledge and Eqs. (1), (3), and (8) as well into account, it can be concluded that the impulse response $h(t, \tau)$ consists of the clutter and noise Eq. (2) and a periodical signal $h_0(t, \tau)$. The signal $h_0(t, \tau)$ due to the respiratory motion of a person has a DC component (depending on d_0) and period $T_b = 1/f_b$. The frequency of its fundamental harmonic component is $f_b \in B$, where $B = \langle 0.2 \text{ Hz}, 0.7 \text{ Hz} \rangle$.

The abovementioned comments summarizing the detailed analyses presented in Refs. [2, 3] indicate that a static person can be detected based on the detection of a periodical signal components of the radargram $h(t, \tau)$ corresponding to a periodical motion with frequency $f_b \in B$ with regard to the slow-time variable (τ) for a constant fast-time instant (t_0). If such a component is detected for $t = t_0$, then the bistatic range of the target (i.e. the length of the trajectory distance $Tx\text{-}target\text{-}Rx$) is ct_0 . And finally, if a proper number of bistatic ranges of the target for the properly defined positions of Tx and Rx are estimated, then the target coordinates can be estimated, for example, by a trilateration or multilateration method.

As it follows from the previous paragraph, the key element of the static person detection consists in the detection of the periodical components of the radargram with the frequency from the interval $B = \langle 0.2 \text{ Hz}, 0.7 \text{ Hz} \rangle$. Here, it should be stressed that the target echo to-noise-and clutter ratio (SNCR) and is usually low. The target detection and then its localization can be onward complicated by a complex environment where the target is situated (strong attenuation due to obstacle, multipath electromagnetic wave propagation, shadowing effect, narrowband interference due to wireless communication systems, etc.). Therefore, there are no simple solutions to be applied for static person detection and localization. The published solutions differ in their approach to clutter and noise suppression, to power spectrum estimation, and to target detection methods. Moreover, there are only a few papers dealing not only with the person detection but also with person localization. The state-of-the art in this field is shortly outlined in the next section.

3. Static person detection and localization: state-of-the art

During the last decade, a variety of the papers intent on human being detection by UWB sensors have been published. These contributions were initially focused mainly on UWB sensor system construction and on basic principle of human being detection (e.g. [5, 6]). Then, the research in the field of UWB sensor systems was devoted also to the development of UWB radar signal processing methods to be applied for moving and static person detection and localization. As we have shown in the previous section, the basic principle of the static person detection consists in the spectrum analyses of the radargram. This fact allows modifying the

methods originally designed for static person detection for estimation of the breathing and heart-beating rate (e.g. [3, 7]). In the next section, we deal with the problem of radar signal processing for the detection and localization of static person only.

This section briefly highlights the approaches and the outcomes of the research in the detection and localization of the static persons but also points out their respective deficiencies, which altogether give ground for motivation of the research presented herein.

Deep analyses of the problem of the human beings detection based on the detection of their respiratory motions have been provided in Refs. [2, 8]. In these works, a very useful model of raw radar data has been introduced. It has been shown that the raw radar data can be modeled as an additive mixture of signal of interest (target echo), stationary and nonstationary clutter, jamming and random noise. What is important, the components of the target echo along the slow-time axis are represented by periodical signals with the fundamental harmonic located in the frequency interval $B = \langle 0.2\text{Hz}, 0.7\text{Hz} \rangle$. The further analyses of the raw radar data have shown that target echo to-noise and clutter ratio SNCR is usually very small. Therefore, the process of the static person detection can be decomposed at least into two phases, which include clutter and noise suppression and spectrum analyses of the radargrams with the suppressed clutter and noise.

The approach chosen for respiratory motion detection proposed in Refs. [8, 9] is divided into three stages: stationary-clutter removal (range-profile subtraction, mean subtraction, linear-trend subtraction), SNCR improvement (filtering in range dimension, slow-time frequency-domain windowing, and nonstationary-clutter suppression by singular value decomposition (SVD)), and threshold-based decision- and range-estimation stage (results of SVD decomposition processing). For the power spectrum estimation, discrete Fourier transform (DFT) is applied. The proposed approach has been successfully demonstrated for the detection of a single person located under rubble.

On the other hand, a bit simpler approach for a static person detection has been introduced in Refs. [2, 5]. In these papers, an exponential averaging and DFT or Welch periodogram has been proposed for background subtraction and power-spectrum estimation, respectively. The obtained results have shown that also this alternative approach can be successfully used for the static person detection under some scenarios.

The analyses of some several other contributions (e.g. [2, 4, 10, 11]) have shown that moving target indicator method (MTI), SVD, combination of correlation analyses and a Curvelet transformation, and CLEAN algorithm can be used for the SNCR improvement. Besides conventional methods of spectrum analyses (e.g. DFT or Welch periodogram), the application of some new methods for the detection of the periodical components of radargram has been proposed. The methods such as Hilbert-Huang transformation (e.g. [11, 12]), S-transform (e.g. [13]), MUSIC algorithm (e.g. [7]) and wavelet transformation and wavelet entropy (e.g. [14]) can be rated among them. The fundamentals of Hilbert-Huang transformation, S-transform, and MUSIC methods can be found in Refs. [15–17], respectively.

The results of the detection phase are represented usually by two-dimensional (2D) figures expressing a propagation rate (fast-time) versus a frequency axis (respiration rate), where high-

level components (so-called “hot spots”) of these figures indicate a presence of the targets. It means that the output of these methods cannot provide any information about target coordinates. In order to localize the static person, their bistatic range or TOA has to be estimated and associated and only then the target can be localized using a proper localization method.

The mentioned approach has been applied in Refs. [18, 19]. In this papers, a sensor network of bistatic UWB radars for multiple person localization was described. The signal processing procedure described in these studies consists of SNCR improvement (using a simple variant of MTI), detection (a power-spectrum estimator application), initial screening (it is conducted via frequency analysis of the detected signals), data association and parameter estimation (maximum likelihood observation-target association technique) and target localization (including determination of number of the target). The sensor network presented in Ref. [18] provides not only very good localization of a set of static persons for a line-of-sight scenario, but it provides the estimation of the frequency of their breathing, too.

The present short but comprehensive review of some papers devoted to the static person detection and localization indicate that there are only a few papers (e.g. [18, 19].) dealing with the problem of multiple static person localization. In order to fill this gap, an approach for multiple person localization based on the detection of their respiratory motion and employing a single UWB sensor only will be introduced in the next section.

4. WP-STAPELOC method

Taking into account the model of raw radar signal $h(t, \tau)$, the basic principle of static person detection introduced in Section 2, and the findings summarized in the previous section as well, the static persons can be localized using the following procedure of UWB sensor signal processing. The procedure consists of a set of phases of signal processing such as background subtraction, target echo enhancement, target detection, TOA estimation and TOA association, and target localization, where each phase is implemented by proper methods of signal processing. As it will be shown later, the detection of persons' respiratory motions is the key phase of the procedure. The input signal of the detectors employed in this phase will be formed using power spectrum of the radargram components. Because Welch periodogram will be used for the estimation of the mentioned power spectrum, the signal processing procedure for static person localization introduced in this section will be referred as WP-STAPELOC method (a method for STAtic PErson LOCalization based on power-spectrum estimation using Welch Periodogram).

In the next paragraphs of this section, the importance and implementation of the particular phases of WP-STAPELOC method will be presented. With the intention to provide a bit deeper insight into the procedure, the importance of its particular phases, the performance of the signal processing methods applied within these phases and the performance of the WP-STAPELOC method as a whole will be illustrated using the experimental data obtained by measurements intent on through-the-wall localization of three static persons using UWB sensor system (the so-called illustrative scenario). Following the outlined concept of this

section, the illustrative scenario will be first described, and then the particular phases of WP-STAPELOC method will be introduced.

4.1. Illustrative scenario

The illustrative scenario was intent on through-the-wall localization of three static persons using an UWB sensor. The measurement scheme for the illustrative scenario is outlined in **Figure 2**. The monitored area was represented by the basement room. The UWB sensor (radar) was situated behind the structural concrete wall of thickness 0.5 m (**Figure 2**). Three persons to be localized stood in the positions P1, P2, and P3. The only observable movements of the persons to be localized were their respiratory motions.

The raw radar data analyzed in this contribution were acquired by means of M-sequence UWB radar systems equipped with one transmitting and two receiving horn antennas (**Figure 3**). The radar antenna positions are outlined in **Figure 2**. The distance between T_x and R_{xi} for $i = 1,2$ was set to 0.45 m. The system clock frequency and operational bandwidth of the applied UWB sensor were 4.5 GHz and DC-2.25 GHz, respectively. The order of the M-sequence emitted by the radar was nine, that is, the impulse response covers 511 samples regularly spread over 114 ns. Then, the unambiguous range of the UWB radar was about 17 m.

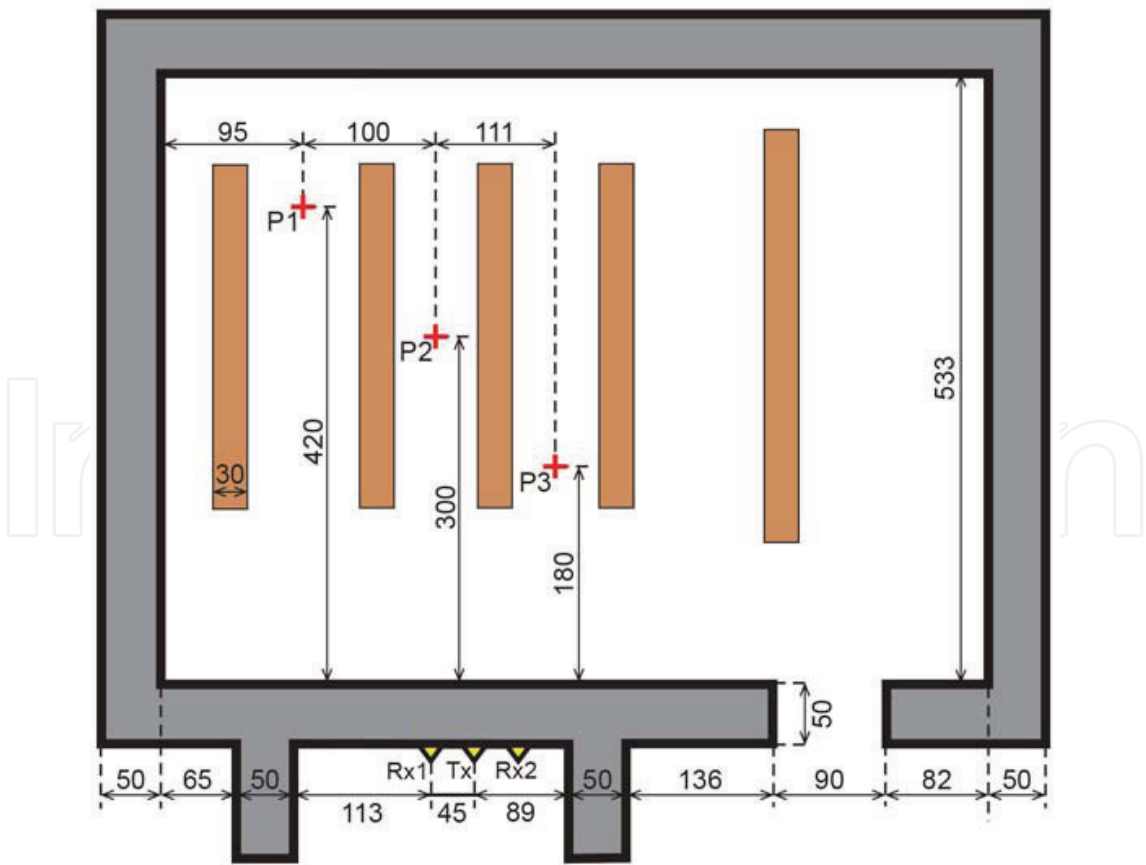


Figure 2. Measurement setup.



Figure 3. UWB radar system.

The radar measurement rate was approximately 13.5 impulse responses per second. The total length of the measurement was 74 s, which corresponds to 1000 impulse responses. The total power transmitted by the particular radar was about 1 mW.

The raw radar data obtained for the illustrative scenario are given in **Figures 4** and **5**. The strongest components identified in these figures correspond to the direct waves between T_x and R_{xi} (the so-called antenna coupling) and the reflections due to the wall. Unfortunately, the target-echo levels are too small, and hence no reflections due to persons are visible in **Figures 4** and **5**. These figures demonstrate very clearly that a further processing of the radargram is necessary to detect and localize the persons. In the next paragraph of this section, we describe WP-STAPELOC method, which can be applied for that purpose.

4.2. Phases of WP-STAPELOC method

As has been stated at the beginning of this section, the WP-STAPELOC method is UWB radar signal processing procedure consisting of the set of the five signal processing phases such as background subtraction, target-echo enhancement, target detection, TOA estimation and TOA association, and target localization, where each phase is implemented by proper methods of signal processing. Now, the particular phases will be presented in the next paragraphs of this section.

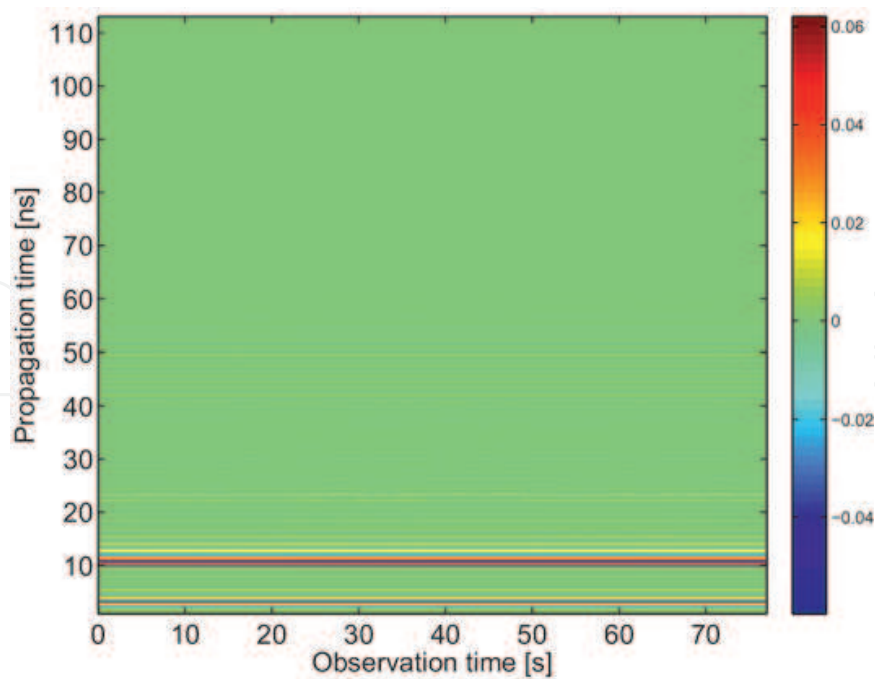


Figure 4. Raw radar data. Receiving channel Rx1.

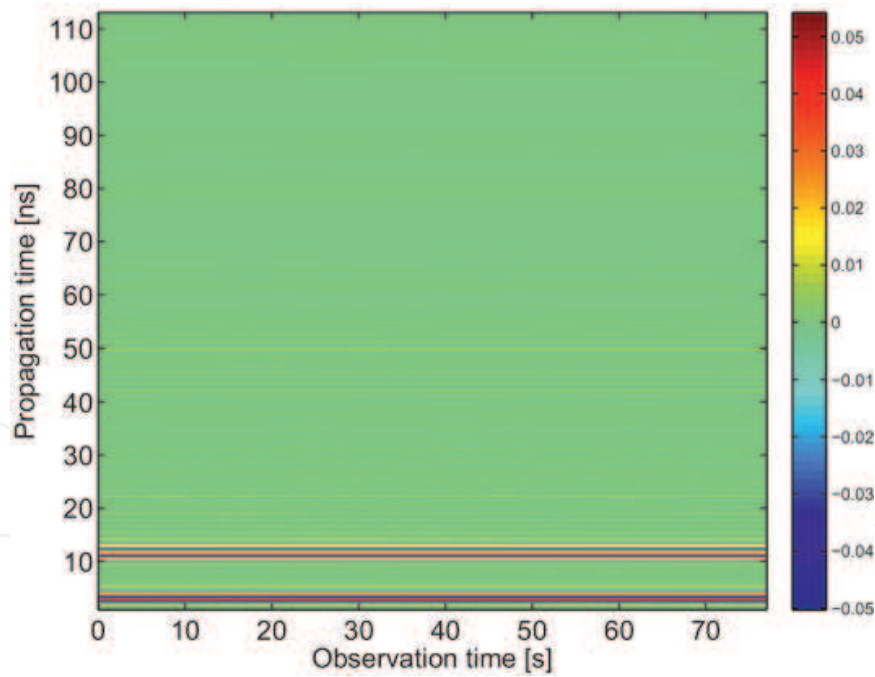


Figure 5. Raw radar data. Receiving channel Rx2.

4.2.1. Phase 1: background subtraction

The analysis of raw radar data has shown that it is impossible to directly identify any static persons in the obtained radargrams. This effect is due to the very small ratio of the

signals reflected by a target (nonstationary components of the radargram) to noise and clutter (stationary components of radargram mainly due to reflections of electromagnetic waves from static objects). In order to detect a target, this ratio has to be increased. For that purpose, background subtraction methods can be used. In Ref. [20], a variety of methods of the background estimation and subtraction have been described. The mentioned methods differ in relation to assumptions concerning the clutter properties, as well as by their computational complexity and convenience for online signal processing. Because of a good performance, high robustness, and low computational complexity, the method of exponential averaging belongs to the most popular and often used methods of background subtraction [20]. According to this method, the background estimate $\hat{b}(t, \tau)$ is obtained by

$$\hat{b}(t, \tau) = \alpha \hat{b}(t, \tau-1) + (\alpha-1)h(t, \tau), \quad 0 < \alpha < 1 \quad (10)$$

where α is a constant weighting factor setting the length of background estimator memory. Then, the radargram with a subtracted background can be obtained by the expression

$$h_b(t, \tau) = h(t, \tau) - \hat{b}(t, \tau) \quad (11)$$

The radargrams with the subtracted background for the illustrative scenario considered in this chapter are given in **Figures 6** and **7**, respectively. Three high-level artifacts similar to lines parallel to the slow-time axis are located in the interval $\langle 20 \text{ ns}, 40 \text{ ns} \rangle$ of fast-time axis. These high-level signals represent the components of the radargram due to static persons.

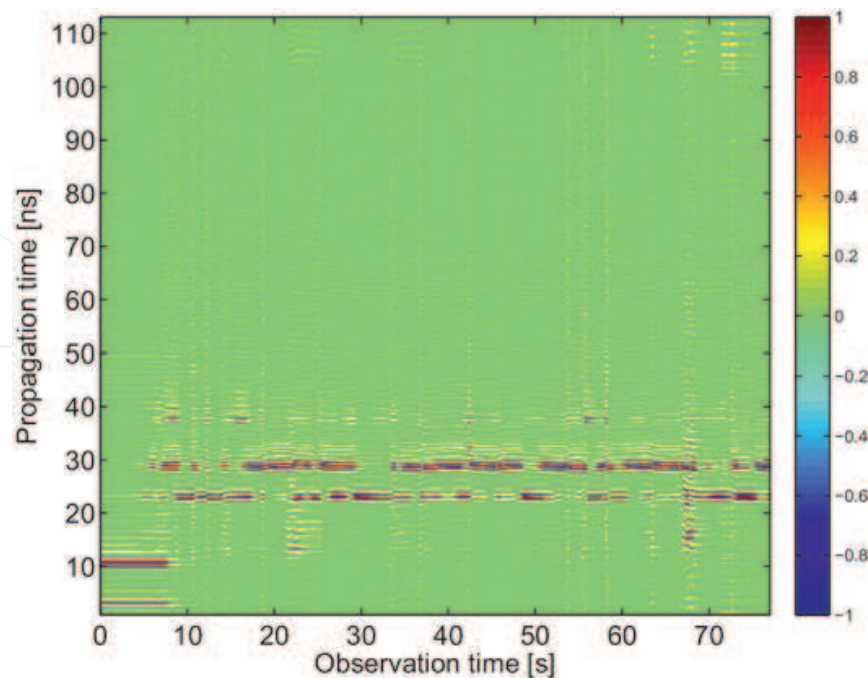


Figure 6. Radargram with subtracted background. Receiving channel Rx1.

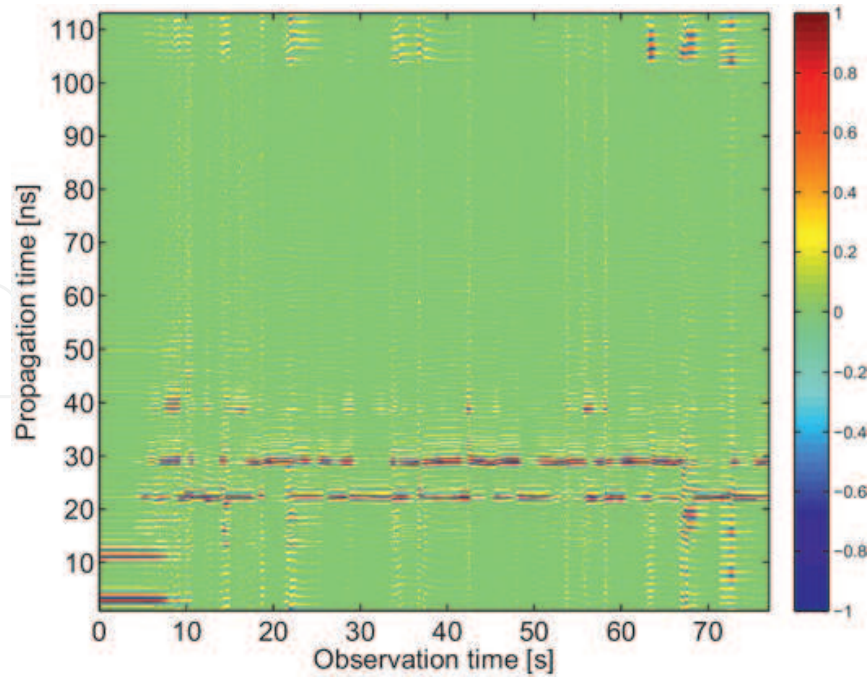


Figure 7. Radargram with subtracted background. Receiving channel Rx2.

4.2.2. Phase 2: target echo enhancement

SNCR can be improved using not only a background subtraction method but also a proper method of the target echo enhancement. An interesting approach for the improvement of SNCR with the special stress for the static person detection has been presented in, for example [8]. Here, the analyses of the impulse responses obtained at monitoring of a static person have shown that the target echo is located within frequency band 0.4–1.4 GHz. Then, filtering in the range dimension (i.e. along fast-time axis) by a proper pass-band filter can be used for low-level echo enhancement. The filter of that kind is sometimes also referred to as a range filter.

As we mentioned above, the key part of the WP-STAPELOC method consists in the power-spectrum estimation of the radargram components $h(t, \tau)$ for the constant values of t (i.e. for $t = t_k$). This condition expresses the fact that the power spectrum will be estimated only for those radargram components due to objects that have the same bistatic range with regard to Tx and Rx (i.e. the distance Tx -target-Rx). It is well known from the spectrum estimation theory that in the case of the estimation of spectral components, which we like to detect (in our case, spectral components from the frequency band $B = \langle 0.2\text{Hz}, 0.7\text{Hz} \rangle$), the spectrum estimator performance depends usually on useful signal-to-noise ratio. Therefore, it would be helpful to increase this ratio before the spectrum estimator application. Following this idea, we propose to filter the signal $h(t_k, \tau)$ by a bandpass filter along the slow-time axis. The passband of this filter should be properly selected taking into account the frequency band $B = \langle 0.2\text{Hz}, 0.7\text{Hz} \rangle$ (signal components due to static persons) and the rate of measurement (i.e. frequency sampling of $h(t, \tau)$ along slow-time axis). In the next, a filter applied for this purpose will be referred to as a slow-time filter. The response of this filter will be denoted as $h_2(t, \tau)$.

In the case of the illustrative scenario, the low cutoff frequency of the T_x and R_{xi} antennas was 750 MHz and the operational bandwidth of UWB sensor was about DC-2.25 GHz. Because the practical operational bandwidth of UWB sensor system (radar device and antennas) used in the illustrative scenario was comparable with the frequency band 0.4–1.4 GHz reported in Ref. [8], no range filtering was applied for low-level echo enhancement. As the slow-time filter, the Caer filter of the second order with the cutoff frequencies 0.1 and 0.8 Hz was applied. The obtained results are presented in **Figures 8** and **9**. If we compare the radargrams with the subtracted background and the corresponding slow-time filter outputs $h_2(t, \tau)$, we can see that the useful signal components (three high-level artifacts similar to lines parallel to slow-time axis located in the interval $\langle 20 \text{ ns}, 40 \text{ ns} \rangle$ of fast-time axis) were enhanced, while some unwanted signal components were suppressed [21].

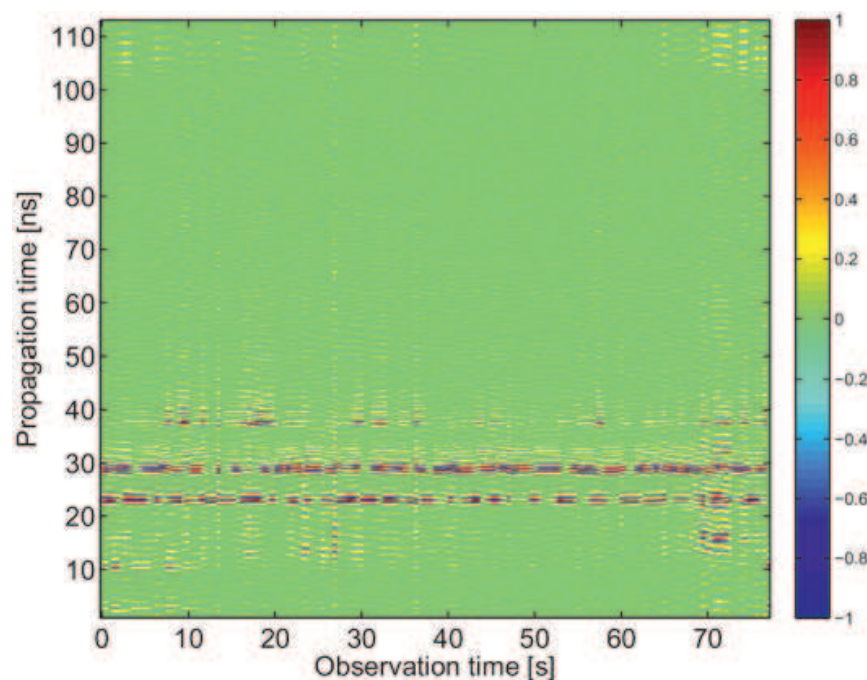


Figure 8. Slow-time filter output. Receiving channel Rx1.

4.2.3. Phase 3: target detection

Detection is the next phase of the radar signal processing procedure, which comes after the background subtraction and the target echo enhancement. Detection methods analyze the radargram with the subtracted background processed by range- and slow-time filters to reach the decision whether a signal scattered by a static person is present or absent in the analyzed radargram. Let the output of Phase 2 be denoted as $h_2(t, \tau)$. According to the conclusion of Section 2, the static person detection can be based on the detection of periodical components of signal $h_2(t_k, \tau)$ (i.e. a constant fast-time instant is considered). For those components, it is necessary to be located in the frequency band $B = \langle 0.2 \text{ Hz}, 0.7 \text{ Hz} \rangle$ and to have a sufficient level of their power as well. The former condition follows from the fact that the frequency band $B = \langle 0.2 \text{ Hz}, 0.7 \text{ Hz} \rangle$ covers the frequencies of human being respiration,

while the latter condition is essential to ensure that we can distinguish between the level of background noise and signal components caused by a static person. Moreover, we have to consider the fact that a person is the so-called distributed target, that is, not the only one but usually several reflections can be received by the sensor from the same person. Then taking into account this knowledge, static persons can be detected by the detector consisting of power-spectrum estimator employing Welch periodogram [17], order statistic constant false alarm rate detector (OS-CFAR) [22] and a simple threshold detector (TD). In the next, this kind of the detector will be referred to as a two-stage detector [23]. Its operation can be described as follows.

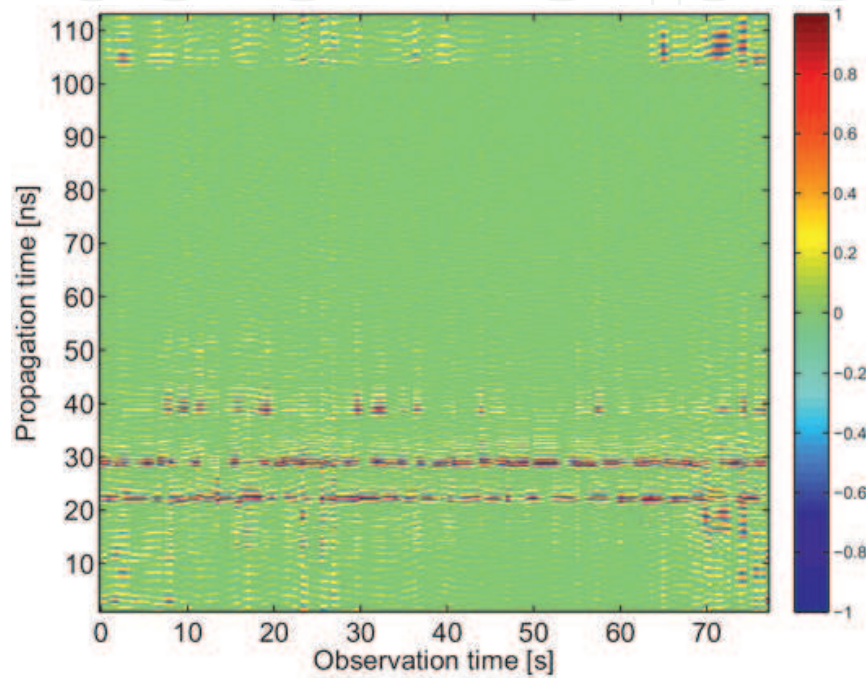


Figure 9. Slow-time filter output. Receiving channel Rx2.

First, the power spectra of the sequences $h_2(t_k, \tau)$ for $\tau \in \langle \tau_1, \tau_2 \rangle$ and for each time instant t_k are estimated using Welch periodogram [17]. Here, we would like to stress that the interval $\langle \tau_1, \tau_2 \rangle$ should be large enough to get a good power-spectrum estimation of the frequency components covering the frequency interval $B = \langle 0.2 \text{ Hz}, 0.7 \text{ Hz} \rangle$. In the next step, the total power of $h_2(t_k, \tau)$ contained in the frequency band $B = \langle 0.2 \text{ Hz}, 0.7 \text{ Hz} \rangle$ denoted as $X_1(t)$ is computed by the integration (summation) of the periodogram components located in this frequency band. Then, the variable $X_1(t_k)$ expresses a measure of the total power of $h_2(t_k, \tau)$ allocated in the frequency interval B including the power of signals reflected by all objects having the bistatic range $d(t_k) = ct_k$ (i.e. the distance $Tx\text{-}object\text{-}Rx$) with regard to the UWB sensor. As we stated before, a significant level of $X_1(t_k)$ indicates that in the bistatic range $d(t_k) = ct_k$ a static person can be located.

With the intention to decide if the level of $X_1(t_k)$ is significant to indicate the presence of a static person, OS-CFAR detector is employed with advantage as the first stage of the two-stage detector. The description of the OS-CFAR is beyond this paper. A reader interested in this topic

can find the detailed description of OS-CFAR detector, for example, in Ref. [22]. The input-output relation of the OS-CFAR can be described by the expression

$$h_1(t) = \begin{cases} 0 & \text{if } X_1(t) \leq \gamma_1(t) \\ 1 & \text{if } X_1(t) > \gamma_1(t) \end{cases} \quad (12)$$

where the level of the threshold $\gamma_1(t)$ is controlled by the OS-CFAR algorithm. The detector output $h_1(t)$ is a binary signal, where "1" ("0") indicates the presence (absence) of the target in the bistatic range $d(t) = ct$.

In the case of person detection by a high-resolution radar, the radar-range resolution is much finer than the size of the target. Then, a human target has to be considered as a distributed target. It means that several reflections due to the same target can be detected. In order to avoid a multiple detection of the same target, the second detection stage is applied within the detection phase. The input signal of this detector denoted as $X_2(t)$ is formed by the sequential summation of $X_1(t_k)$ over the interval with the length V , where V represents approximately the maximum number samples of $h(t, \tau)$ containing the reflections from the same target. Then, the signal $X_2(t)$ can be expressed as follows:

$$X_2(t) = \sum_{l=k}^{k+V-1} h_1(t_l) \quad (13)$$

Now, the operation of the second stage of the detector (TD) can be described by the expression

$$h_2(t) = \begin{cases} 0 & \text{if } X_2(t) \leq \gamma_2 \\ 1 & \text{if } X_2(t) > \gamma_2 \end{cases} \quad (14)$$

where γ_2 is a constant threshold. The TD output $h_2(t)$ is a binary signal, where "1" ("0") indicates the presence (absence) of a static person in the bistatic range $d(t) = ct$. The signal $h_2(t)$ represents also the output of the detection phase.

Now, the performance of the above-described two-stage detector can be illustrated using the data obtained at our illustrative scenario. First, the power spectra of slow-time filter outputs are given in **Figures 10** and **11**. Here, the frequency components due to the static persons located in the frequency band $B = \langle 0.2 \text{ Hz}, 0.7 \text{ Hz} \rangle$ and within the fast-time interval $\langle 20 \text{ ns}, 40 \text{ ns} \rangle$ can be identified. The performance of OS-CFAR detector is outlined in **Figures 12–15**. These figures indicate that OS-CFAR detector is able to detect the static persons (three target detected in the fast-time interval $\langle 20 \text{ ns}, 40 \text{ ns} \rangle$). We can observe also in these figures that several isolated reflections from the same person were detected by OS-CFAR detector. After the application of TD, the number of the detected targets is decreased. Targets are mostly detected in the fast-time interval $\langle 20 \text{ ns}, 40 \text{ ns} \rangle$ (**Figures 16–19**).

As it might be expected, some false alarms can be observed in the OS-CFAR and TD outputs. The total number of the false alarms produced by TD is smaller than that created by OS-CFAR detector. Hence, we can see that TD application decreases the total number of false alarms observed at the output of the detection phase. We will show in the following paragraphs that

these false alarms will be eliminated by the TD output processing within TOA estimation and TOA association phase.

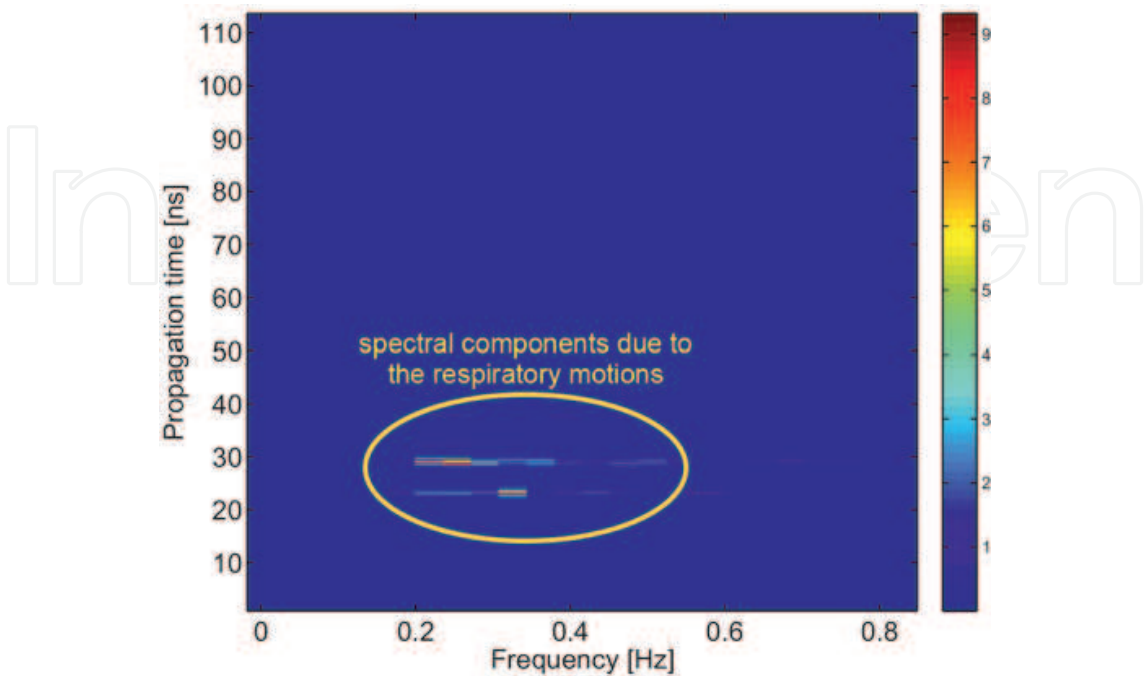


Figure 10. Power spectrum of slow-time filter output. Receiving channel Rx1.

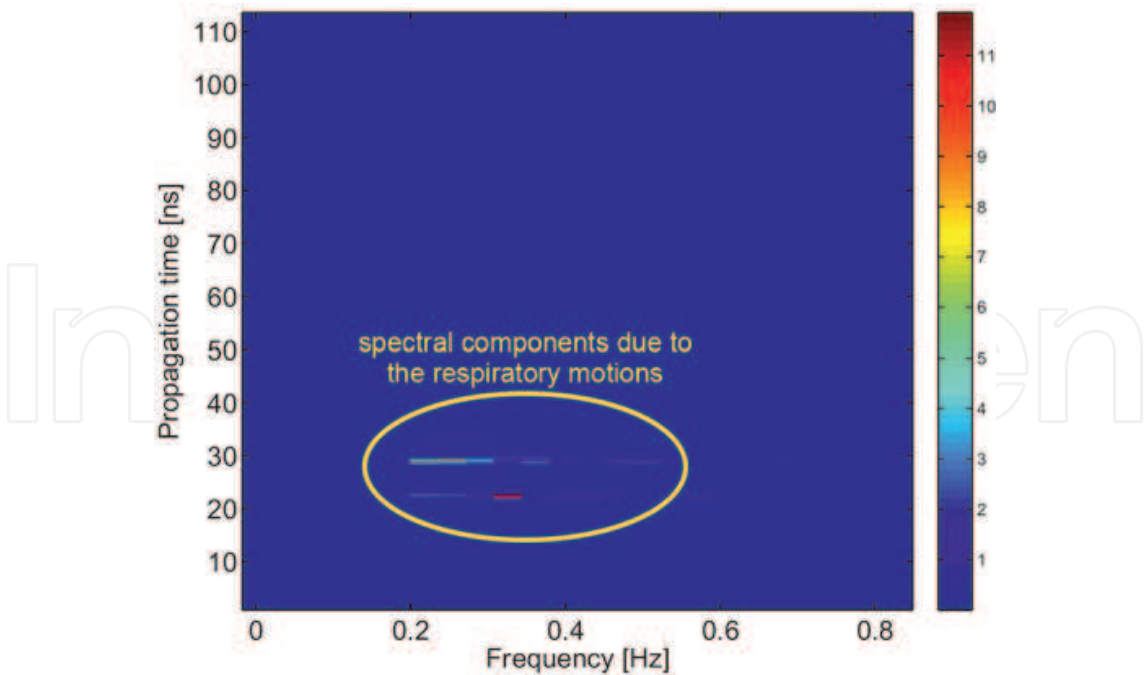


Figure 11. Power spectrum of slow-time filter output. Receiving channel Rx2.

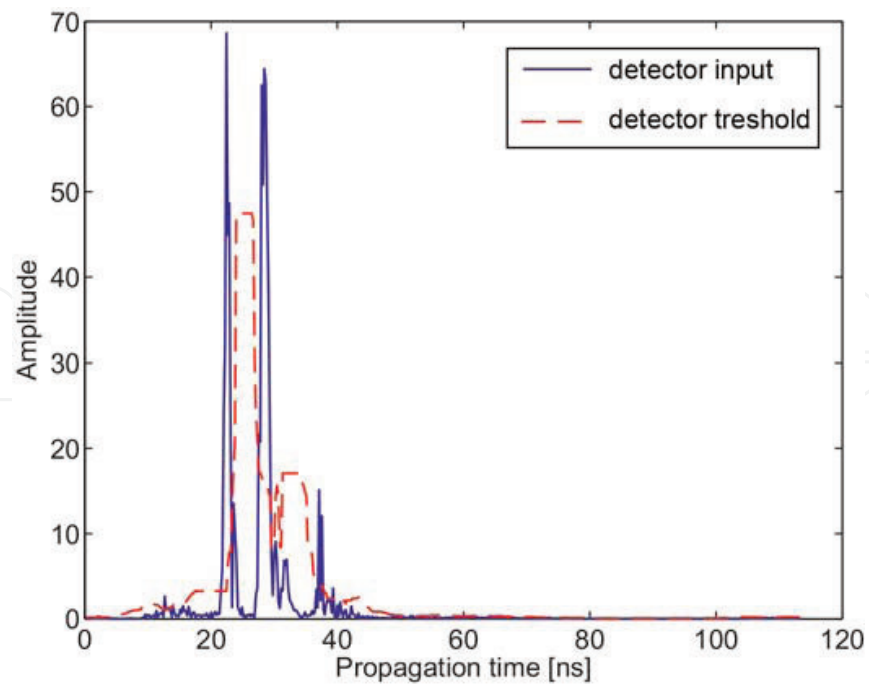


Figure 12. Total power of the signal $h_2(t_k, \tau)$ allocated in the frequency band $B(X_1(t))$, blue color) and OS-CFAR detector threshold ($\gamma_1(t)$, red color). Receiving channel Rx1.

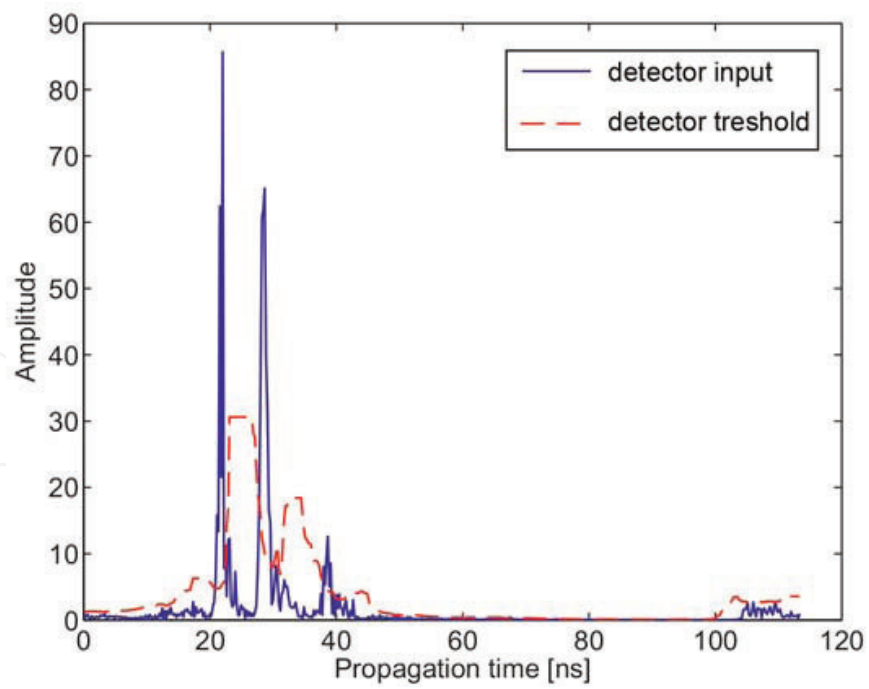


Figure 13. Total power of the signal $h_2(t_k, \tau)$ allocated in the frequency band $B(X_1(t))$, blue color) and OS-CFAR detector threshold ($\gamma_1(t)$, red color). Receiving channel Rx2.

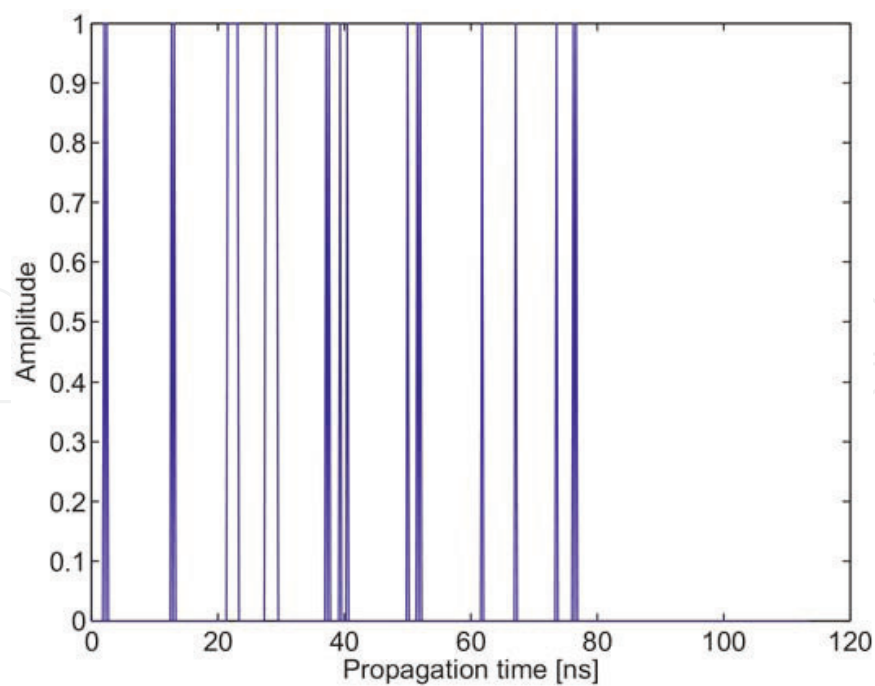


Figure 14. OS-CFAR detector output. Receiving channel Rx1.

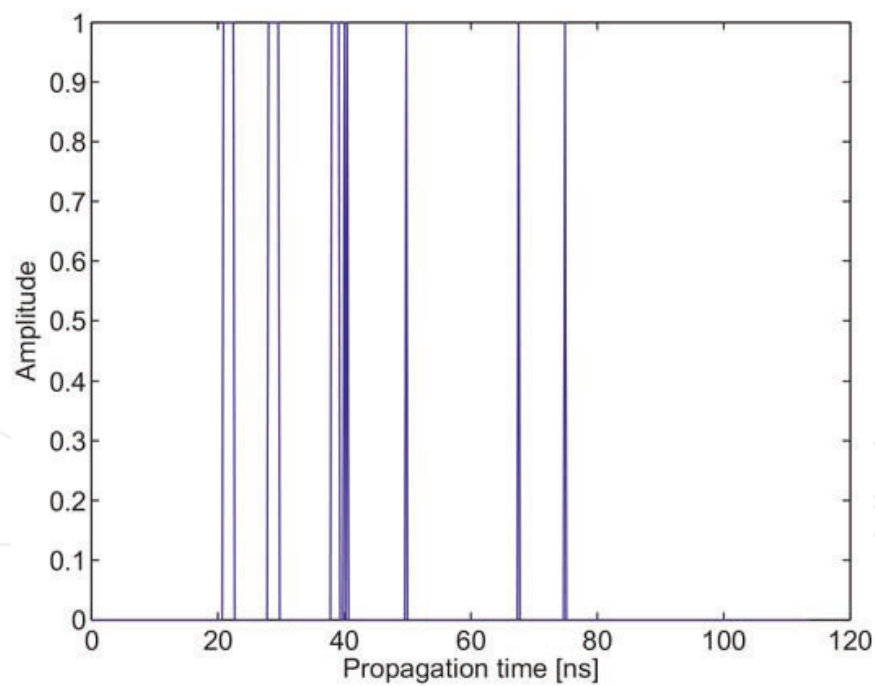


Figure 15. OS-CFAR detector output. Receiving channel Rx2.

4.2.4. Phase 4: TOA estimation and TOA association

The very efficient algorithm for TOA estimation can be found, for example, in Ref. [24]. This algorithm referred to as the trace connection method provides not only TOA estimation but

also the association of the data received from two receiving channels and deghosting operation essential for multiple target detection. The trace connection method is quite complex, and hence it is beyond this paper. The details concerning this method can be found, for example, in Ref. [24]. The output of this phase consists in the pairs of TOA associated with the same target obtained for the first (Rx1) and second (Rx2) receiving channel of the radar.

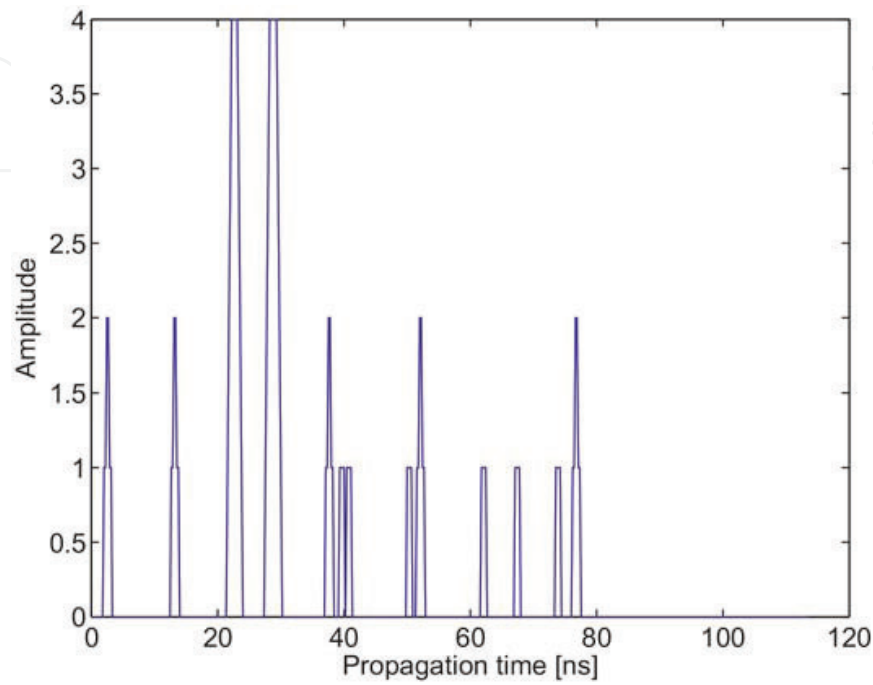


Figure 16. TD input. Receiving channel Rx1.

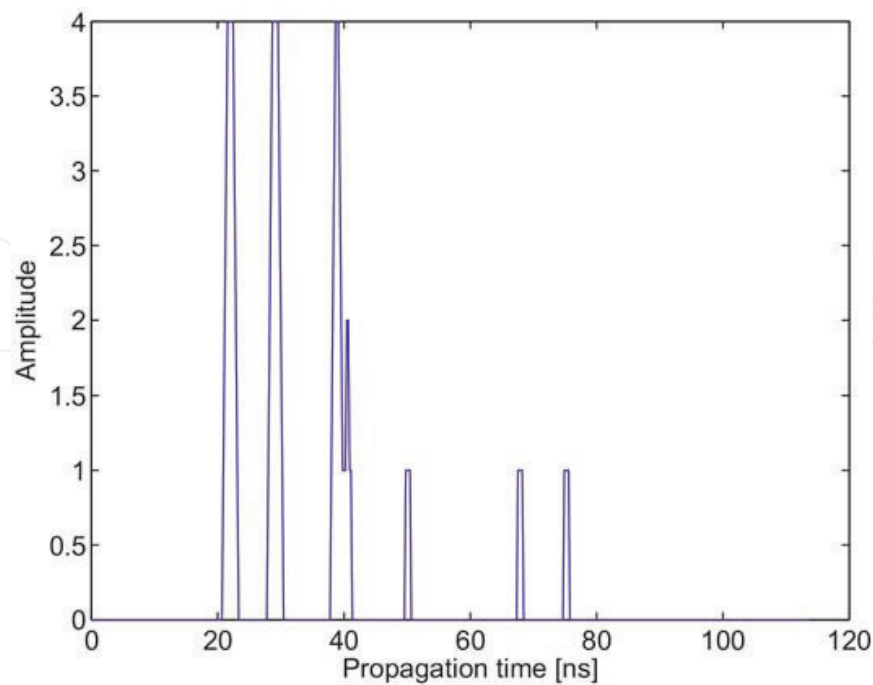


Figure 17. TD input. Receiving channel Rx2.

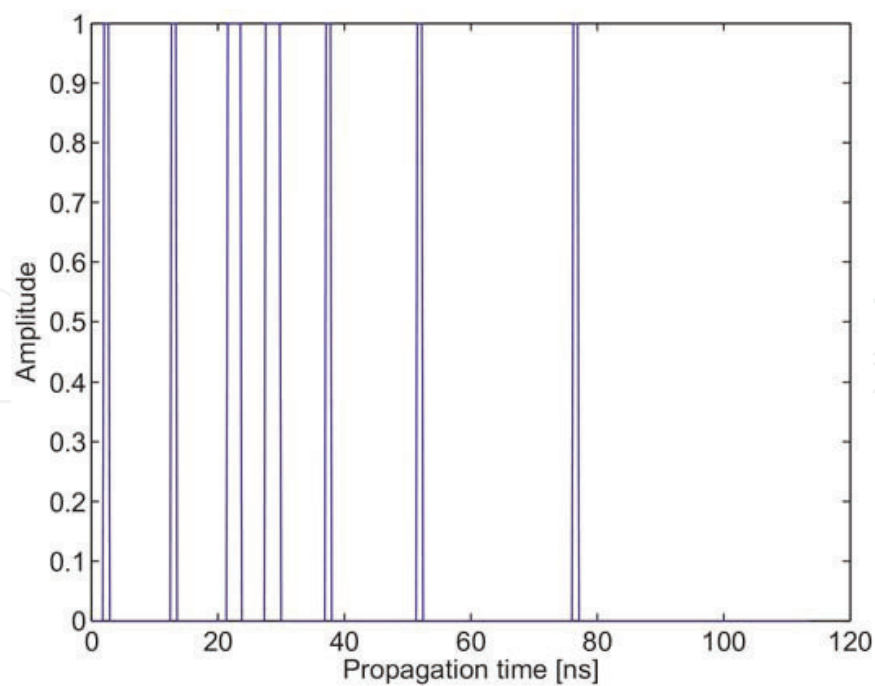


Figure 18. TD output. Receiving channel Rx1.

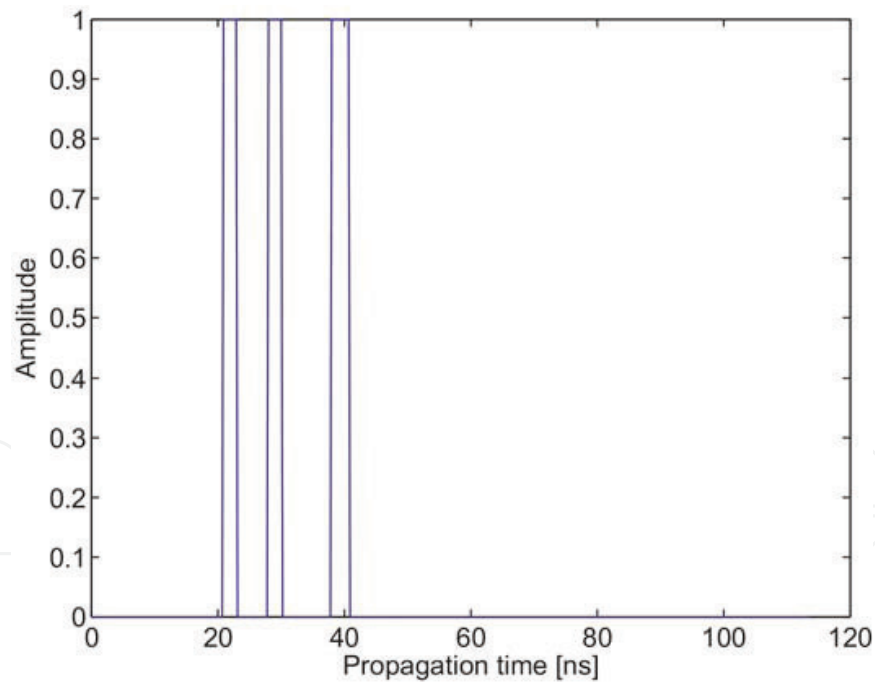


Figure 19. TD output. Receiving channel Rx2.

4.2.5. Phase 5: target localization

The estimations of the target coordinates represent the output of the target localization phase and at the same time the final result of WP-STAPELOC method. The results provided by the trace connection method (Phase 4) and by direct computation method (Phase 5) for the

illustrative scenario discussed throughout this paper are given in **Figure 20**. Here, the true and estimated positions of the static persons are expressed by green and red marks, respectively. Moreover, tolerance areas represented by the circles with the center in the true position of the target and with the diameter 30 cm are also sketched in **Figure 20**. The tolerance areas are used to demonstrate that the person is not a pointed but distributed target with a certain non-zero size. The results depicted in **Figure 20** confirm that WP-STAPELOC method performs very well for the illustrative scenario. In spite of the complex scenario (three-person localization through the thick concrete wall), all static persons were localized with the good accuracy (all persons were localized in corresponding tolerance area).

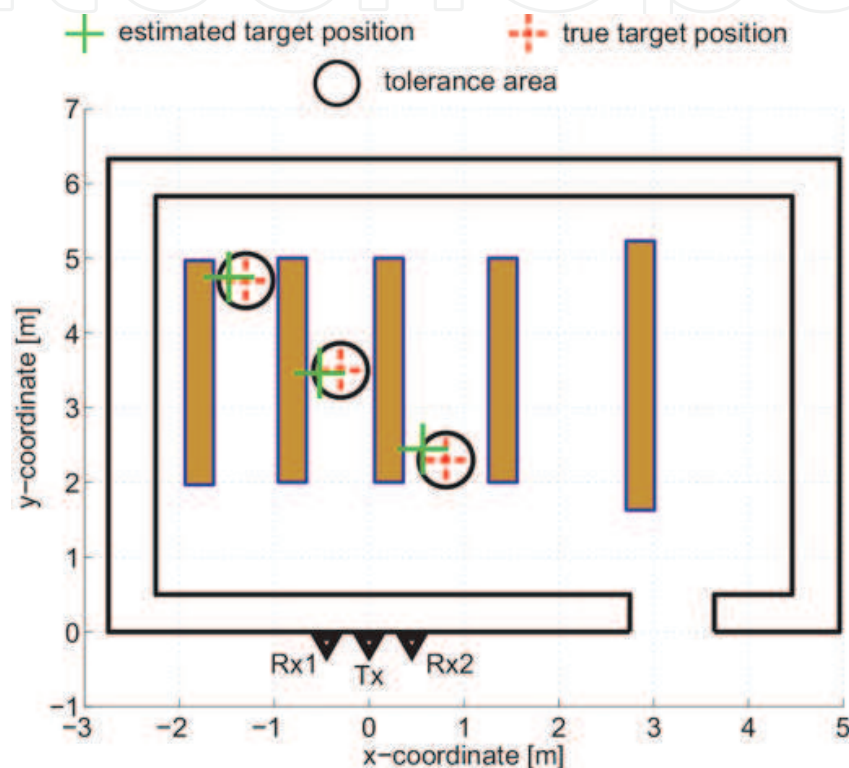


Figure 20. True (green mark) and estimated (red mark) positions of the static persons.

5. Conclusion

In this chapter, we have dealt with a problem of multiple static person localization using a single M-sequence UWB radar. For that purpose, we have introduced the novel radar signal processing procedure focused on the static person detection and localization. The key novelty of this method consists of the application of a two-stage detector based on the combination of power-spectrum estimator, OS-CFAR detector, and a simple TD. The performance of the proposed procedure has been evaluated for through-the-wall scenario of localization of three static persons. The obtained results have confirmed that the procedure described in this paper can provide a good performance also for challenging scenarios.

Unfortunately, the illustrated good performance of the WP-STAPELOC method does not mean that this method is able to provide a perfect and robust performance almost for all possible

scenarios. Nevertheless, the presented approach addresses the core problems of multiple static person localization and suggests their fundamental solutions. This fact is considered of the highest importance and benefits of the proposed methods. In order to obtain a really robust system for the localization of static persons by UWB sensors, a modified version of WP-STAPELOC method has to be developed. The new modified version based on the presented principles should take into account shadowing effect, wall effect and its compensation, multipath electromagnetic wave propagation, a presence of strong reflectors in monitored area, narrowband interference, and so on. Moreover, the static person localization method should be optimized with regard to its computational complexity. We believe that the solution of this challenging and complex task will be available in the near future.

Acknowledgements

This work was supported by the Slovak Research and Development Agency under the contract No. APVV-0404-12.

Author details

Dušan Kocur*, Daniel Novák and Mária Švecová

*Address all correspondence to: dusan.kocur@tuke.sk

Department of Electronics and Multimedia Communications, Technical University of Košice, Košice, Slovakia

References

- [1] Huffmann C., Ericson L. Through-the-wall sensors for law enforcement. market Survey. [Internet]. 10/2012 [Updated: 04/2014]. Available from: <https://www.ncjrs.gov/pdffiles1/nij/grants/245944.pdf> [Accessed: 25.8.2016]
- [2] Sachs J., Helbig M., Herrmann R., Kmec M., Schilling K., Zaikov E. Remote vital sign detection for rescue, security, and medical care by ultra-wideband pseudo-noise radar. *Ad Hoc Networks*. 2014;13:42–53. DOI: 10.1016/j.adhoc.2012.07.002
- [3] Lazaro A., Girbau D., Villarino R. Techniques for clutter suppression in the presence of body movements during the detection of respiratory activity through UWB radars. *Sensors*. 2014;14(2):2595–2618. DOI: 10.3390/s140202595
- [4] Singh S., Liang Q., Chen D., Sheng L. Sense through wall human detection using UWB radar. *EURASIP Journal on Wireless Communications and Networking*. 2011;20:1–11. DOI: 10.1186/1687-1499-2011-20

- [5] Zaikov E., Sachs J., Aftanas M., Rovňáková J. Detection of trapped people by UWB radar. In: Microwave Conference (GeMIC), 2008 German; 10–12 March 2008; VDE VERLAG GmbH; 2008. pp. 1–4.
- [6] Yarovoy A. G., Ligthart L. P., Matuzas J., Levitas B. UWB radar for human being detection. IEEE Aerospace and Electronic Systems Magazine. 2006;21(3):10–14. DOI: 10.1109/MAES.2006.1624185
- [7] Rivera N. V., Venkatesh S., Anderson Ch., Buehrer R. M. Multi-target estimation of heart and respiration rates using ultra wideband sensors. In: Signal Processing Conference, 2006 14th European; 4–8 September 2006; Florence, Italy; IEEE; 2006. pp. 1–6.
- [8] Nezirović A. Trapped-Victim Detection in Post-Disaster Scenarios using Ultra-Wideband Radar [dissertation]. Delft: Delft University of Technology; 210. 165 p. Available from: <http://repository.tudelft.nl/islandora/object/uuid:4416dd48-9829-4af0-b678-8fcd8e87788a/?collection=research>
- [9] Nezirović A., Yarovoy A. G., Ligthart L. P. Signal processing for improved detection of trapped victims using UWB radar. IEEE Transactions on Geoscience and Remote Sensing. 2010;48(4):2005–2014. DOI: 10.1109/TGRS.2009.2036840
- [10] Li X., Liang Q., Lau F. Sense-through-wall human detection using the UWB radar with sparse SVD. Physical Communication. 2014;13:260–266. DOI: 10.1016/j.phycom.2013.12.002
- [11] Li J., Liu L., Zeng Z., Liu F. Simulation and signal processing of UWB radar for human detection in complex environment. In: Ground Penetrating Radar (GPR), 2012 14th International Conference; 4–8 June 2014; Shanghai, China; IEEE; 2012. pp. 209–213. DOI: 10.1109/ICGPR.2012. 6254862
- [12] Liu Z., Liu L., Barrowes B. The application of the Hilbert-Huang transform in through-wall life detection with UWB impulse radar. PIERS Online. 2010;6(7):695–699. DOI: 10.2529/PIERS100217122115
- [13] Li J., Zeng Z., Sun J., Liu F. Through-wall detection of human being's movement by UWB radar. IEEE Geoscience and Remote Sensing Letters. 2012;9(6):1079–1083. DOI: 10.1109/LGRS.2012.2190707
- [14] Wang Y., Yu X., Zhang Y., Lv H., Jiao T., Lu G., et al. Using wavelet entropy to distinguish between humans and dogs detected by UWB radar. Progress in Electromagnetics Research. 2013;139:335–352. DOI: 10.2528/PIER13032508
- [15] Huang N., Shen Z., Long S., Wu M., Shih H., Zheng Q. The empirical mode decomposition and the Hilbert spectrum for nonlinear and non-stationary time series analysis. Proceedings of the Royal Society of London A: Mathematical, Physical and Engineering Sciences. 1998;454(1971):903–995. DOI: 10.1098/rspa.1998.0193
- [16] Stockwell R. G., Mansinha L., Lowe R. P. Localization of the complex spectrum: The S-transform. IEEE Transactions on Signal Processing. 1996;44(4):998–1001. DOI: 10.1109/78.492555

- [17] Proakis J. G., Manolakis D. G. Digital Signal Processing. 4th ed. Michigan University: Pearson Prentice Hall; 2007. 1084 p.
- [18] Kim Ch., Lee J. ToA-based multi-target localization and respiration detection using UWB radars. EURASIP Journal on Wireless Communications and Networking. 2014;2014(1):1–15. DOI: 10.1186/1687-1499-2014-145
- [19] Kim C., Lee J., Cho T., Ki D., Cho B. H., Yoon J. Multi-target localization of breathing humans. In: Proceedings of the 2013 IEEE International Conference on Ultra-Wideband (ICUWB 2013); Sydney, Australia; 2013. pp. 49–54.
- [20] Rovňáková J., Švecová M., Kocur D., Nguyen T. T., Sachs J. Signal processing for through wall moving target tracking by M-sequence UWB radar. In: Radioelektronika, 2008 18th International Conference; 24–25 April 2008; Prague, Czech Republic.; IEEE; 2008. p. 1–4. DOI: 10.1109/RADIOELEK.2008.4542694
- [21] Kocur D., Švecová M., Rovňáková J. Through-the-wall localization of a moving target by two independent ultra wideband (UWB) radar systems. Sensors. 2013;13(9):11969–11997. DOI: 10.3390/s130911969
- [22] Rohling H. Some radar topics: waveform design, range CFAR and target recognition. In: Byrnes J., Ostheimer G., editors. Advances in Sensing with Security Applications. 2nd ed. Springer, Netherlands; 2006. pp. 293–322. DOI: 10.1007/1-4020-4295-7_13
- [23] Novák D., Kocur D. Multiple static person localization based on respiratory motion detection by UWB radar. In: 2016 26th International Conference Radioelektronika (RADIOELEKTRONIKA); 19–20 April 2016; Košice. IEEE; 2016. pp. 252–257. DOI: 10.1109/RADIOELEK.2016.7477386
- [24] Rovňáková J., Kocur D. TOA estimation and data association for through-wall tracking of moving targets. EURASIP Journal on Wireless Communications and Networking. 2010;2010(1):1–11. DOI: 10.1155/2010/420767